Suspended electrode kinetics of mechanically activated pyrite[①]

YIN Zhou-lan(尹周澜), ZOU Jian-peng(邹俭鹏), CHEN Qi-yuan(陈启元), ZHANG Ping-min(张平民)
(College of Chemistry and Chemical Engineering, Central South University,
Changsha 410083, China)

[Abstract] Suspended electrode was firstly used to study the mechanically activated pyrite . It is found that the dissolved oxygen in the solution has much influence on the suspended pyrite electrode by comparing the open circuit potential of suspended electrodes at different atmosphere conditions. From the measurements of anodic quasi-stable polarization of the suspended electrode, the transfer coefficients of anodic reaction process of activated pyrite and unactivated pyrite β are equal to 0. 136 and 0. 202 respectively in 1 mol•L^{-1} KCl deoxygenation electrolyte system at 25 ℃.

[Key words] mechanical activation; suspended electrode; voltammetry; quasi-stable polarization
[CLC number] TF 01; O 646. 21   [Document code] A

1 INTRODUCTION

Mechanical activation is widely applied in enhancing metallurgical process[1~3] and chemical synthesis[4,5]. So far it is difficult to ascertain which factor affecting the mechanical activation process is the most important. The enhancement mechanism of mechanical activation remains in a stage of the established physical modeling[6,7] and no more essential progress has obtained. The activation behaviour of mechanically activated pyrite is studied by electrochemical kinetics of constructing suspended electrode in this paper.

2 EXPERIMENTAL PREPARATIONS

2. 1 Mineral materials

Large pieces of pure specimen pyrite from Hunan Geological Museum, P. R. China, was used in the experiment. Pyrite was immersed in 5% diluted HCl solution for about 12 h. Then it was washed by pipe water and distillated water subsequently and dried. After that, pyrite was broken to less than 1mm approximately to avoid the mechanical activation and was put into the desiccator for about three months. Samples below 38 mesh were used as unactivated pyrite and samples over 38 mesh as mechanically activated ones. Contents of Fe and S in pyrite by chemical quantitative analysis were shown in Table 1 and contents of impurities by emission spectrum analysis

Table 1 Content of Fe and S in pyrite

Element	Mass fraction/ %
Fe	45. 63
S	52. 38

in Table 2.

2. 2 Examination of electrochemical workstation

A conventional three-electrode cell was used with platinum plates as the auxiliary and working electrodes and a saturated KCl calomel electrode as the reference electrode. The electrochemical cell was put in a container where water was recycled through a super-thermostat to maintain its temperature at 25 ℃. The reliability of the CHI660A electrochemical workstation(Shanghai, China) was examined by voltammetry method with $K_4Fe(CN)_6$/ $K_3Fe(CN)_6$ normal electrochemical system.

Table 2 Contents of impurities in pyrite

Element	Mass fraction/ %	Element	Mass fraction/ %
Si	0. 1	As	0. 03
Ca	0. 01	Zn	0. 05
Sn	0. 01	Co	0. 005
Sb	0. 01	Ni	0. 001

The voltammetric experiments were performed in the electrolyte consisting of 0. 5 mol/ L $K_3Fe(CN)_6$ and 0. 4 mol/ L KNO_3 at a sweeping rate of 10 mV/ s. $E_{p, a} - E_{p, c} \approx 59$ mV and $i_{p, a} \approx i_{p, c}$ were concluded from the voltammetric curves. According to the relationship between sweeping rate and anodic peak current, the diffusion coefficient of $Fe(CN)_6^{3-}$ was calculated from Randles-Sevcik equation as $D_{Fe(CN)_6^{3-}} = 5. 21 \times 10^{-6}$ cm^2•s^{-1} which is coincided with the literature value of $5. 60 \times 10^{-6}$ cm^2•s^{-1}[8].

3 EXPERIMENTAL

3. 1 Open circuit potential

Three-electrode system was also used in the suspended cell as shown in Fig. 1. In the experiments, the agitator maintained a constant rotating rate in 100 mL of 1 mol·L^{-1} KCl solution with 200 g of pyrite at (25 ±1) ℃. The potential values in the present paper was measured vs. saturated KCl calomel electrode at 25 ℃.
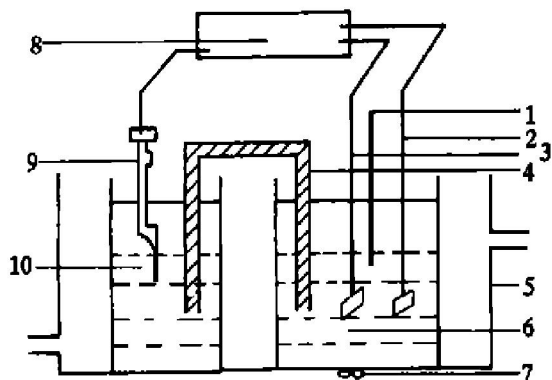

Fig. 1　Device of pyrite suspended cell
1 —N$_2$ pipe; 2 —Pt electrode; 3 —Pt electrode;
4 —Salt bridge; 5 —thermostat; 6 —1 mol·L^{-1} KCl solution;
7 —Agitator; 8 —Electrochemical workstation;
9 —Saturated potassium chloride calomel electrode;
10 —Saturated KCl solution

Deoxygenation was carried out with blowing 99. 99% nitrogen continuously. The open circuit potentials of activated and unactivated pyrite suspended electrode at different atmosphere conditions are shown in Fig. 2.

The open circuit potential can be regarded as the mixed potential of suspended electrode. It can be seen from Fig. 2 that the open circuit potential of activated pyrite is obviously lower than that of unactivated one and becomes stable more easily with time prolonged, which inferres that the oxidation ability of pyrite is increased through mechanical activation. Fig. 2 also shows that the dissolved oxygen in the solution has a great effect on the suspended pyrite electrode.

3. 2　Anodic quasi-stable polarization curve

99. 99% nitrogen was inputted to the electrolyte for about 30 min to remove O$_2$ which has a great effect on the suspended pyrite electrode as mentioned above.

Experiments were carried out by quasi-stable polarization method with suspended electrode as working electrode at a sweeping rate of 8 mV/s in 1 mol·L^{-1} KCl electrolyte. The results are shown in Fig. 3.

It is shown from Fig. 3 that the anodic oxidation current can be detected obviously at φ> 0. 8 V for activated pyrite suspended electrode and at φ> 0. 95 V for unactivated one, which indicates that the activated pyrite suspended electrode is more easily oxided. One possible reason is that 3d electrons initially filled in t$_{2g}$ molecular orbital of the mechanically activated pyrite is more easily stimulated by the action of external electric field[9].

It was discovered from the experiments that bubbles emerged from the working electrode in 1 mol·L^{-1} KCl blank solution when anodic potential attained to 1. 15 V. Cl$_2$ was detected in the oxidation process as the product since it made the humid amylum KI test paper blue. Therefore the first peak in Fig. 3 is caused by the oxidation of pyrite suspended electrode and the second by the evolution of Cl$_2$.

It was found in the experiments that pH of the percolated solution was 3. 6 after several continuous sweepings when the unactivated pyrite suspended electrode system was percolated immediately. Fe^{3+} and SO$_4^{2-}$ were not detected in the percolated solution since the solution did not change to red when detected by 1% KSCN and no white precipitate was observed when BaCl$_2$ was added to the solution. Fe^{2+} was ascertained because the percolated solution turned to red rapidly when detected by 2% 2, 2'-pyridine alcohol solution. Small amount of S was also analyzed by quantitative analysis. Therefore the oxidation process of pyrite suspended electrode can be deduced as FeS$_2$ − 2e= Fe^{2+} + 2S according to the chemical analysis.

The relationship between potential and polarization current of activated pyrite suspended electrode was shown in Table 3.

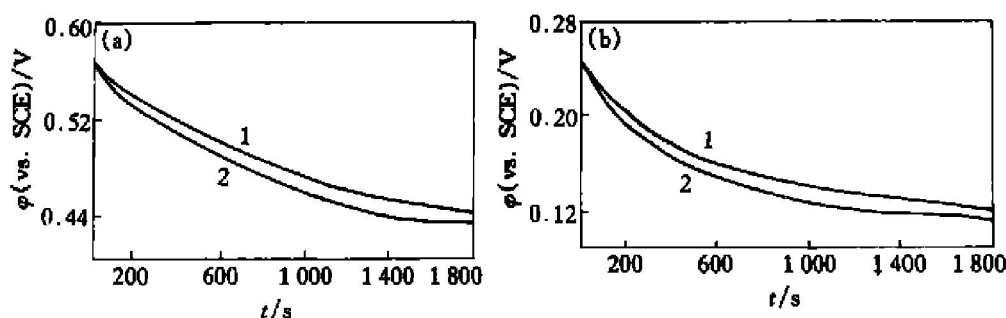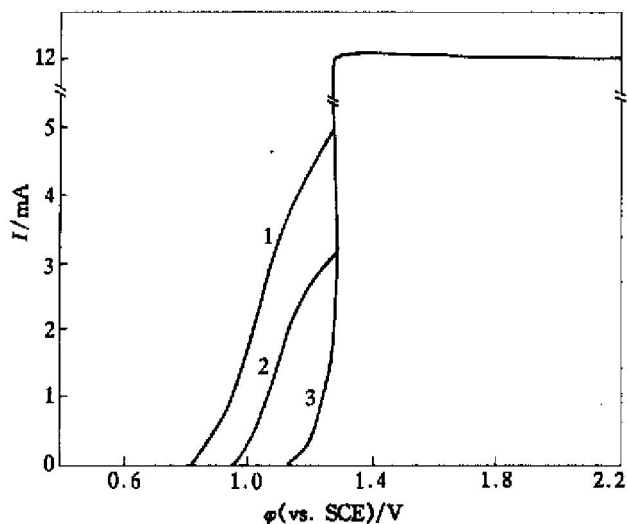The lg$I$- φ curve presented a satisfactory linear

Fig. 2　Open circuit potential in different suspended electrode systems
1 —Air; 2 —Nitrogen; a —Unactivated pyrite; b —Activated pyrite

Table 3　Relationship between potential and
polarization current

I/mA	lg(I/mA)	$\varphi_{electrode}$/V
0.79	– 3.102	0.91
1.21	– 2.917	0.95
2.0	– 2.7	0.99
2.8	– 2.553	1.01
3.81	– 2.419	1.07

Fig. 3　Quasi-stable polarization curves of
suspended electrode
1 —Activated pyrite; 2 —Unactivated pyrite;
3 —KCl blank solution

relationship in the range of 0.9~ 1.1 V as shown in Fig. 4. The regressive equation is $\varphi = 1.57991 + 0.21069$ lg$I$ and its regressive coefficient R is 0.98238.
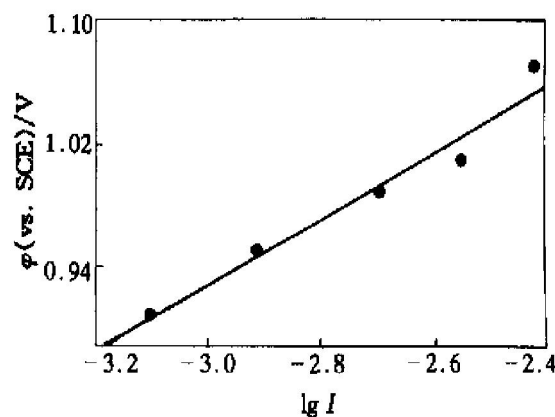
According to Tafel equation[10]:

$$\eta = -\frac{2.3RT}{\beta nF}\lg J_0 + \frac{2.3RT}{\beta nF}\lg J$$

$$= -\frac{2.3RT}{\beta nF}\lg J_0 + \frac{2.3RT}{\beta nF}\lg \frac{I}{A}$$

$$= -\frac{2.3RT}{\beta nF}\lg(AJ_0) + \frac{2.3RT}{\beta nF}\lg I$$

and

$$\eta = \varphi - \varphi_{eq}$$

$$\varphi = [-\frac{2.3RT}{\beta nF}\lg(AI_0) + \varphi_{eq}] + \frac{2.3RT}{\beta nF}\lg I$$

β is calculated to be 0.136 for activated pyrite suspended electrode and 0.202 for unactivated pyrite suspended electrode as n is 2 from the reaction equation of the suspended electrode.


Fig. 4　Relationship between φ and lg$I$

3.3　Voltammetry

The voltammetry curves of activated and unactivated pyrite suspended electrodes are shown in Fig. 5. The forward and backward curves of pyrite suspended electrode are overlapped approximately in the voltametry experiments when the sweeping rate is changed from 5~ 100 mV·s^{-1}. The agreement of coincidence of the forward and backward curves is better at lower sweeping rates. Therefore the whole anode process is controlled by electrochemical reaction. It is also found from Fig. 5 that the oxidation activity of activated pyrite is higher than that of unactivated pyrite since larger current passes through the activated pyrite suspended electrode at the same electrode potential.

4　CONCLUSIONS

1) The dissolved oxygen in the solution has a
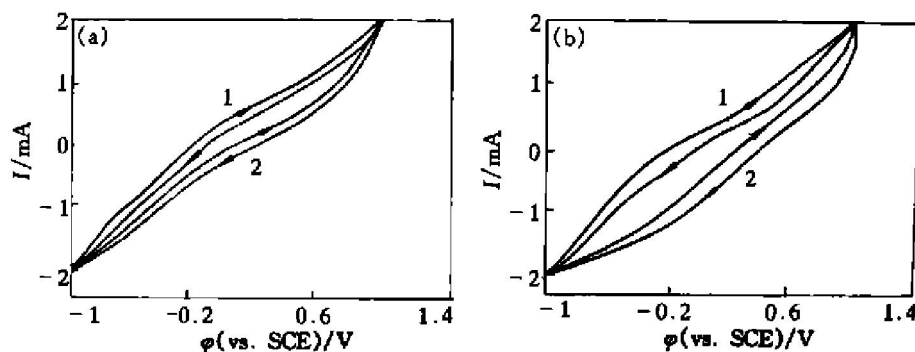
Fig. 5　Vltammetric curve of suspended electrode
(a) —10 mV/s; (b) —60 mV/s; 1 —Activated pyrite; 2 —Unactivated pyrite

great effect on the suspended pyrite electrode by comparing the open circuit potential of suspended electrode at different atmosphere conditions.

2) The activated pyrite suspended electrode is more easily oxidated than the unactivated pyrite suspended electrode. The anode process of pyrite suspended electrode is controlled by electrochemical reaction.

3) The transfer coefficients β of anodic reaction process of activated pyrite and unactivated pyrite are calculated to be 0. 136 and 0. 202 respectively in $1 \, mol \cdot L^{-1}$ KCl deoxygenation electrolyte system at 25 ℃.

ACKNOWLEDGEMENT

[REFERENCES]

[1]   Balaz P. Influence of solid state properties on ferric chloride leaching of mechanically activated galena [J] . Hydrometallurgy, 1996, 40(3) : 359– 368.

[2]   Tromans D, Meech J A. Enhanced dissolution of minerals: microtopograph and mechanical activation [J] . Minerals Engineering, 1999, 12(6) : 609– 625.

[3]   JIA Cheng-chang, LIU Xiao-yang, XIE Zi-zhang, et al. Preparing tungsten alloys with mechanically activated powder [J] . Journal of Tinghua University, 1999, 39 (6) : 35– 38.

[4]   JIANG Ji-sen, GAO Lian, YANG Xie-long, et al. Mechanochemical synthesis of nanocrystalline zinc ferrite [J] . Chemical Journal of Chinese Universities, 1999, 20 (1) : 1– 4.

[5]   Stojanov B D, Pavlonic V B, et al. Dielectric properties of barium-titants sintered from tribophysically activated powders [J] . J Eur Ceram Soc, 1999, 20(1) : 1– 4.

[6]   Boldyrev V V. Mechanical Activation of Minerals [M] . Amsterdam: Elsevier. 1989: 103.

[7]   Tkacova K. [J] . International Journal of Mineral Processing, 1993, 40: 17– 31.

[8]   ZOU Jin-yun. Research on measuring electrochemical kinetic parameters through rotating disc electrode [J] . Materials Conservation, 1980, 3: 18– 21.

[9]   ZHAO Zhong-wei. Study on the mechanochemistry and leaching of auriferous sulfide concetrates [D] . Central South University of Technology, 1995.

[10]   ZHA Quan-xing. Treatise of Electrode Process Kinetics [M] . Beijing: Science Publishing Press, 1987.

(Edited by ZHU Zhong-guo)